NEUROSCIENCE

The repertoire of CSF antiviral antibodies in patients with neuroinflammatory diseases

Yoshimi Enose-Akahata[1], Limin Wang[2], Fahad Almsned[3], Kory R. Johnson[3], Yair Mina[1], Joan Ohayon[4], Xin Wei Wang[2], Steven Jacobson[1]*

Multiple sclerosis (MS) is a chronic inflammatory demyelinating disease of the central nervous system (CNS). Although various viruses have been proposed to contribute to MS pathology, the etiology of MS remains unknown. Since intrathecal antibody synthesis is well documented in chronic viral infection and neuroinflammatory diseases, we hypothesized whether the patterns of antigen-specific antibody responses associated with various viral exposures may define patients with CNS chronic immune dysregulation. The pan-viral antibody profiling in cerebrospinal fluid (CSF) and serum of patients with MS showed significant differences from those in healthy volunteers and a pattern of antibody responses against multiple viruses, including the previously identified Epstein-Barr virus. These findings demonstrate that virus-specific antibody signatures might be able to reflect disease-associated inflammatory milieu in CSF of subjects with neuroinflammatory diseases.

INTRODUCTION

Multiple sclerosis (MS) is a chronic neurodegenerative inflammatory disease of the central nervous system (CNS), leading to demyelination and progressive neurological disability (*1*). The etiology of MS is still unknown and is multifactorial, involving genetic and environmental factors (*2*). A hallmark of MS is the detection of oligoclonal immunoglobulin G (IgG) bands and increased antibody-secreting B cells in the cerebrospinal fluid (CSF) that are associated with long-term B cell survival in this compartment (*3*). Although the cause of this B cell expansion is poorly understood, B cell depletion clinical interventional strategies including rituximab and ocrelizumab are approved therapies for MS (*4*), supporting a role for B cells in the pathogenesis of MS.

To date, a number of infectious viruses, including measles, mumps, Epstein-Barr virus (EBV), human herpesvirus 6, and other ubiquitous human herpesviruses, have been proposed to contribute to MS pathology, although not one virus has been definitively shown to be the causative agent (*5*). In particular, a link between EBV and MS has long been suspected, and recently, this association has again re-emerged based on recent reports demonstrating increased EBV-specific antibodies in serum of patients with MS (*6*) and clonally expanded B cells in MS cross-reactive for EBV and GlialCam (*7*). However, it is unclear whether antibody responses against EBV are uniquely elevated in MS and what is the extent of EBV reactivity in the CSF of patients with MS. Intrathecal antibody synthesis is well documented in chronic virus-associated neurologic disease with demyelination, neuroinflammation, and persistent immune dysregulation in the CNS (*8*). Viral activation and/or reactivation may be associated with such a dysregulated inflammatory response, leading to a loss of antiviral immunity and viral shedding. In addition, it has been suggested that virus-specific immune responses may cross-react with self-antigens (molecular mimicry), thus contributing to the pathophysiology of the disease. We here hypothesize that if environmental factors including virus infections and immune reactivation against viruses play a role as "triggers" in MS, then antibody signatures against such viral exposures may be defined that represent immunological signatures in patients with MS.

[1]Viral Immunology Section, National Institute of Neurological Disorders and Stroke, National Institutes of Health, Bethesda, MD, USA. [2]Laboratory of Human Carcinogenesis, Center for Cancer Research, National Cancer Institute, National Institutes of Health, Bethesda, MD, USA. [3]Bioinformatics Section, National Institute of Neurological Disorders and Stroke, National Institutes of Health, Bethesda, MD, USA. [4]Neuroimmunology Clinic, National Institute of Neurological Disorders and Stroke, National Institutes of Health, Bethesda, MD, USA.
*Corresponding author. Email: jacobsons@ninds.nih.gov

RESULTS AND DISCUSSION

To identify virus-specific antibody signatures, we tested CSF and paired serum of MS patients and healthy normal volunteers (HVs) using VirScan, an established platform for the comprehensive serologic profiling of the entire known human virome. The technique is based on phage immunoprecipitation sequencing (PhIP-seq) technology that uses a bacteriophage library that displays proteome-wide peptides from a total of 206 known human pathogenic viruses in 56–amino acid peptide tiles with a 28–amino acid overlap between adjacent peptides (n = 105,362) (*9*). This virus-specific antibody profiling methodology has been used to identify various viral infections in human samples such as serum and CSF including human immunodeficiency virus, influenza, dengue, enterovirus, and severe acute respiratory syndrome coronavirus 2 (*9*–*13*). It is the same platform recently used to demonstrate increased anti-EBV serological responses in MS (*6*). Besides detecting specific antiviral antibody responses, VirScan has been used to epitope map a viral exposure signature in humans with hepatocellular carcinoma (*14*). Given the recent interest in VirScan to specifically detect increased antibodies to EBV in MS (*6*), we addressed whether antibody responses to specific viruses versus identification of an antiviral antibody signature could be defined in a cohort of patients with MS. Patients with MS and HVs were matched with age, gender, and race (table S1). We examined virus-specific antibody responses in both serum and matched CSF and included patients with human T lymphotropic virus 1 (HTLV-1)–associated myelopathy/tropical spastic paraparesis (HAM/TSP), a disease with a known viral etiology that resembles clinical features of MS (*15*). HAM/TSP is a chronic progressive

neuroinflammatory myelopathy associated with HTLV-1 infection and chronically activated immune responses due to the infiltration of inflammatory cells into the CNS (*16*). Elevated antibody-secreting B cells with increased HTLV-1–specific antibodies are detected in CSF of patients with HAM/TSP (*17*). After collecting the raw PhIP-seq data of VirScan, we analyzed the data using two pipelines: (i) the antibody binding *Z* score pipeline previously reported (*6*) with the aim to identify the presence of a peptide-specific antibody (viral discovery pipeline) and (ii) an analysis of covariance (ANCOVA) pipeline based on PhIP-seq read counts that tests for and identifies signatures of differential peptides under leave-one-out cross-validation (LOOCV) conditions (viral exposure signature pipeline).

On the basis of the relative abundance of antibody binding against each epitope, VirScan enabled comprehensive, unbiased detection of antibodies against viruses, principal viruses with higher prevalence in humans including herpesviruses and respiratory viruses, in both serum and CSF of all the subjects (Fig. 1). As expected, antibody binding *Z* scores against primate T lymphotropic viruses (PTLVs), which include HTLVs and the simian counterparts (simian T lymphotropic virus), were highly elevated in serum of patients with HAM/TSP but not in HVs and patients with MS, indicating that the assay can identify the etiologic agent in HAM/TSP (Fig. 1, A and B). By contrast, in patients with MS, the overall serum antibody binding *Z* scores against viral peptide tiles were similar with those in HVs, and there was no antibody response against any single virus specific for MS (Fig. 1A). However, consistent with previous reports (*6*), patients with MS compared to HVs showed increased antibody binding *Z* scores against viruses in serum including EBV (described as human herpes virus 4 in Fig. 1A). High antibody binding *Z* scores against human herpesviruses, such as EBV and cytomegalovirus (CMV; described as human herpes virus 5), were detected in serum of patients with HAM/TSP (Fig. 1A). Compared to serum, CSF samples also showed a similar trend of increased antibody binding *Z* scores, with less background, against multiple viruses including herpesviruses and respiratory viruses. The antibody binding *Z* scores against PTLVs were increased in CSF of patients with HAM/TSP but not in HVs and patients with MS, indicating that patients with HAM/TSP had a virus-specific antibody response against HTLV in both serum and CSF (Fig. 1B). High antibody binding *Z* scores against human herpesviruses and respiratory viruses were also detected in CSF of patients with MS and those with HAM/TSP (Fig. 1B). When we compared the number of viral peptide tiles recognized by serum and CSF antibodies in patients with MS to those in HVs, MS patients showed a significant increase in the number of viral peptide tiles including EBV and respiratory syncytial virus (Fig. 1, C and D). However, patients with HAM/TSP also showed significant increases in the number of EBV and CMV peptide tiles and PTLV peptide tiles recognized by antibodies in both serum and CSF of patients with HAM/TSP compared to HVs (Fig. 1, C and D). Our findings demonstrated that although patients with MS showed increased antibody responses associated with EBV peptide tiles in both serum and CSF by VirScan using a *Z*-score analysis pipeline, this may not be specific for MS since increased antibodies against EBV and CMV were also detected in patients with HAM/TSP. This suggests that increased virus-specific immune responses, particularly against ubiquitous human herpesviruses, may be common in patients with neuroinflammatory diseases.

While VirScan has been useful in virus discovery for detecting the presence of virus peptide–specific antibodies (*9*, *13*), we have also used VirScan as an antibody profiling methodology that could identify unique immunological signatures in subjects with chronic virus infection and neuroinflammatory diseases. Using the PhIP-seq read counts in conjunction with ANCOVA under LOOCV conditions, we tested for and identified signatures of differential virus peptide-specific antibodies between patients with MS, HAM/TSP, and HVs. Using machine learning under LOOCV conditions, we demonstrate that these signatures can be leveraged to classify patients respectively (fig. S1). In CSF of patients with MS and those with HAM/TSP, antibodies reactive to a total of 1911 and 972 viral peptide tiles, respectively, were found to be differentially expressed compared to HVs (tables S2 and S3). The magnitude and direction of these viral peptide–specific differences are described by a volcano plot (Fig. 2, A and B). When CSF sample relationships between MS and HVs are inspected by principal components analysis (PCA) using the ANCOVA-corrected counts for the 1911 differentially identified peptide tiles, clear separation is observed across both the first and second components (Fig. 2C). Patients with HAM/TSP also showed clear separation in CSF from HVs by PCA using the ANCOVA-corrected counts for the 972 differentially identified peptide tiles (Fig. 2D). When CSF sample relationships between MS and HVs, and separately for HAM/TSP and HVs, are inspected by clustered heatmap analysis using the ANCOVA-corrected counts for the differentially identified peptide tiles, samples organize into distinct groups (Fig. 2, E and F). These analyses demonstrate that the differential viral peptide tiles identified may represent immunological signatures in CSF for MS and HAM/TSP. When the peptide tiles that comprise each signature are inspected, not one viral species is represented. For the 1911 viral peptide tiles that constitute the MS signature in CSF, a total of 167 viral species are represented, including 55 peptide tiles for EBV (table S4). Fifteen of these 55 EBV peptide tiles, representing BALF2, BcLF1, BFLF1, BFRF2, BHLF1, BPLF1, BTRF1, EBV nuclear antigen 4 (EBNA4), EBNA6, LF2, and latent membrane protein 1 (LMP1), have greater counts in CSF of patients with MS compared to HVs (table S2). For the 972 viral peptide tiles comprising the HAM/TSP signature in CSF, a total of 135 viral species are represented, including 74 peptide tiles in PTLVs (table S5). Of these 74 PTLV peptide tiles, representing Envelope (Env), Gag, Protease (Pro), Polymerase (Pol), HTLV-1 basic leucine zipper domain factor (HBZ), Tax, and open-reading frame II (ORFII), 72 have greater counts in CSF of patients with HAM/TSP compared to HVs (tables S3 and S5). Other viruses represented in the HAM/TSP signature include multiple peptide tiles of EBV and CMV (tables S3 and S5). When machine learning is applied under LOOCV conditions to the MS signature in CSF, patients with MS could be correctly classified 93.33% of the time (fig. S2).

Given the differential antibody patterns identified in CSF between patients with MS or HAM/TSP and HVs, we applied the same methods to analyze the antibody patterns in serum between patients with MS or HAM/TSP and HVs (Fig. 3). As we have shown in CSF, these analyses demonstrate that the differential viral peptide tiles identified represent immunological signatures in serum for MS and HAM/TSP (Fig. 3 and tables S6 and S7). For the 1893 viral peptide tiles comprising the MS signature in serum, not 1 viral species is represented but rather a total of 164

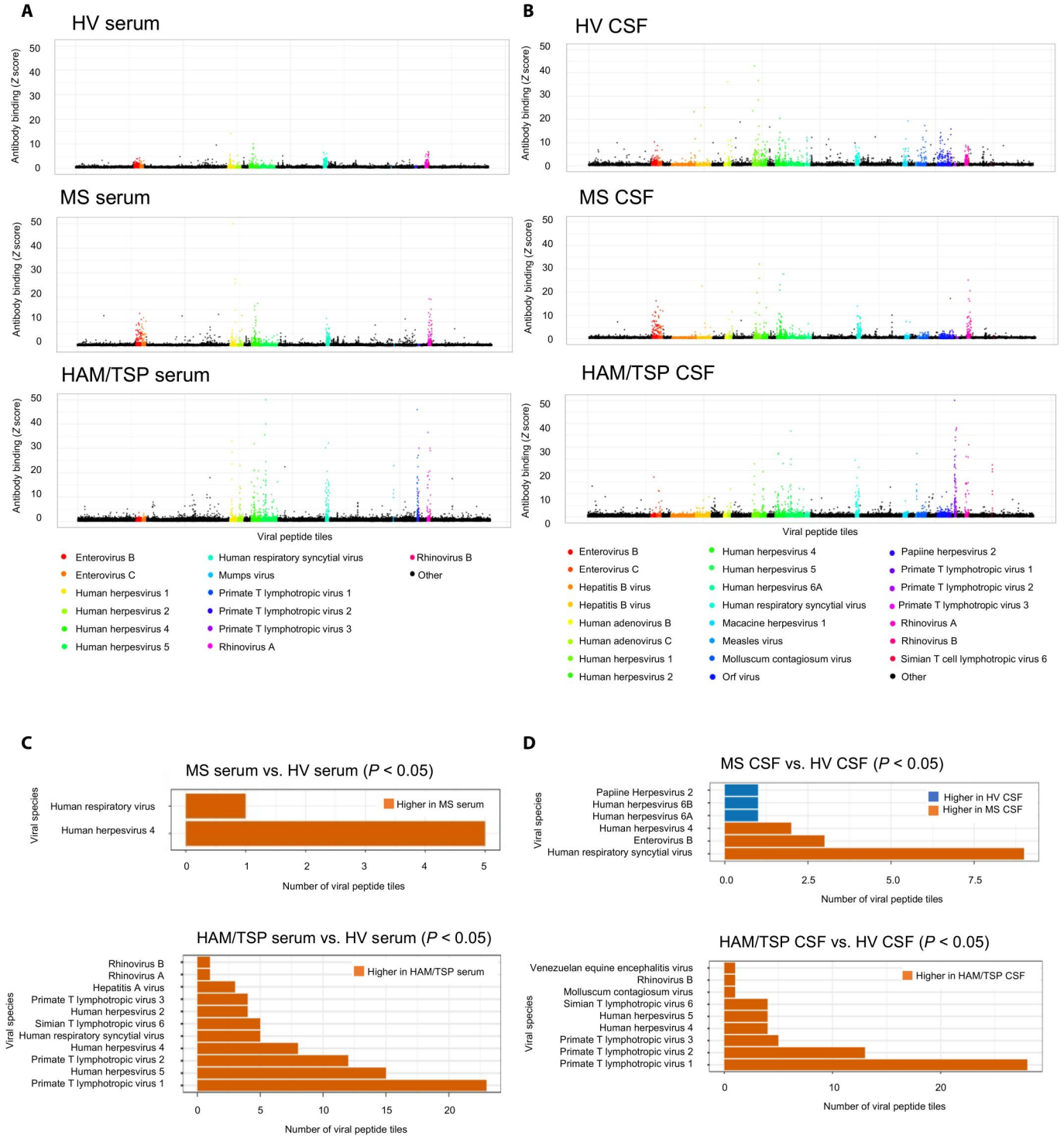

Fig. 1. Detection of antibodies against virus peptide tiles in serum and CSF using VirScan. (**A** and **B**) Scatterplots showing the mean *Z* scores of antibodies against the entire viral peptide tiles in serum (A) and CSF (B) of healthy volunteer (HVs), patients with multiple sclerosis (MS), and patients with HTLV-1–associated myelopathy/tropical spastic paraparesis (HAM/TSP). (**C** and **D**) Number of viral peptide tiles with significantly different antibody binding between patients with MS or HAM/TSP and HVs in serum (C) and CSF (D). Human herpesvirus 1 (known as herpes simplex virus-1); human herpesvirus 2 (known as herpes simplex virus-2); human herpesvirus 4 [known as Epstein-Barr virus (EBV)]; human herpesvirus 5 [known as cytomegalovirus (CMV)].

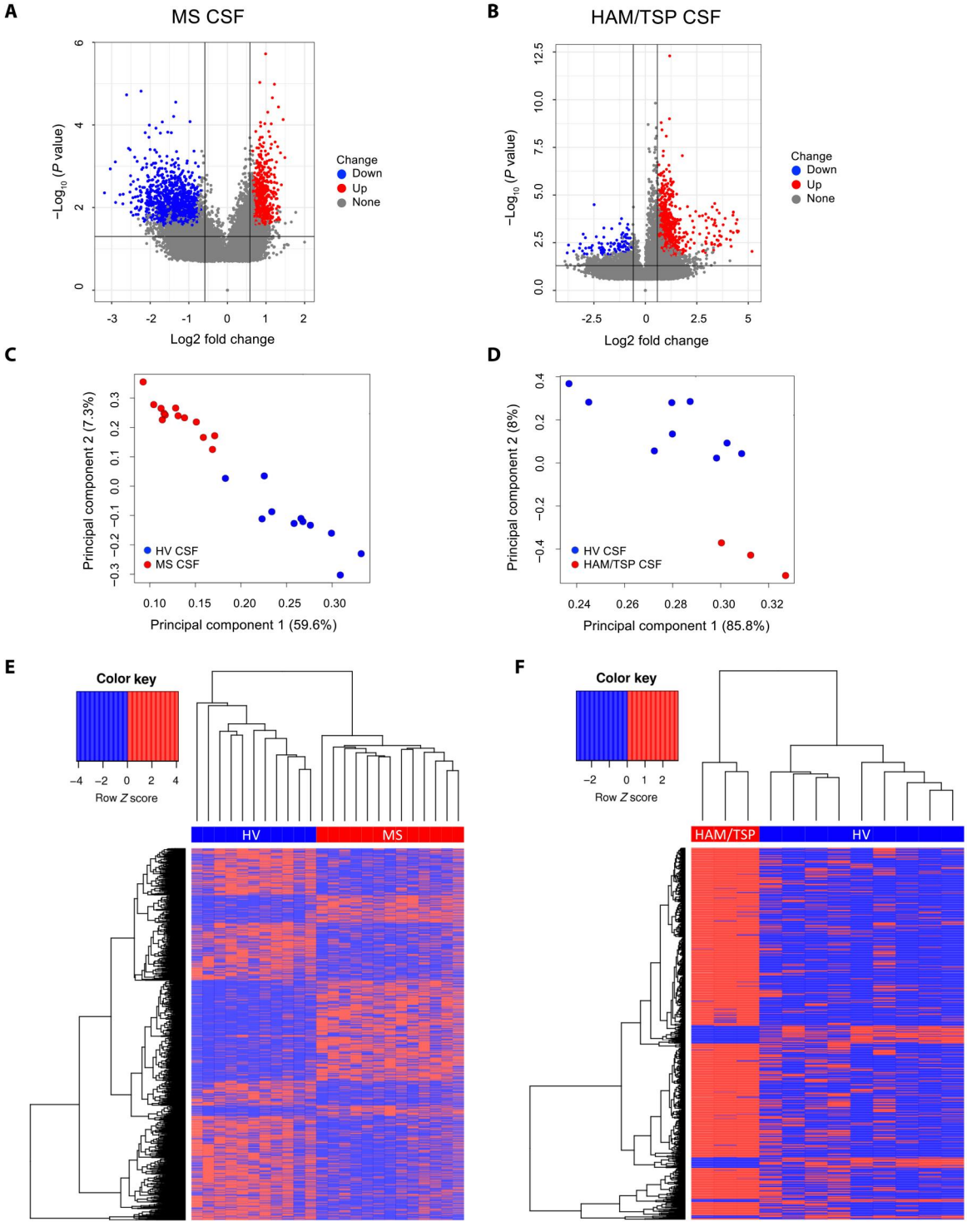

Fig. 2. Differential antibody profiles in CSF between patients with MS and HVs. (**A** and **B**) Volcano plots showing significant fold changes of antibodies against viral peptide tiles in CSF of patients with MS (A) and patients with HAM/TSP (B) compared to HVs. (**C** and **D**) PCA plot showing the significant differences of antibodies against viral peptide tiles in CSF of patients with MS (C) and patients with HAM/TSP (D) compared to HVs. (**E** and **F**) Combined heatmap with cluster analysis showing the significant differences of antibodies against viral peptide tiles in CSF of patients with MS (E) and patients with HAM/TSP (F) compared to HVs.

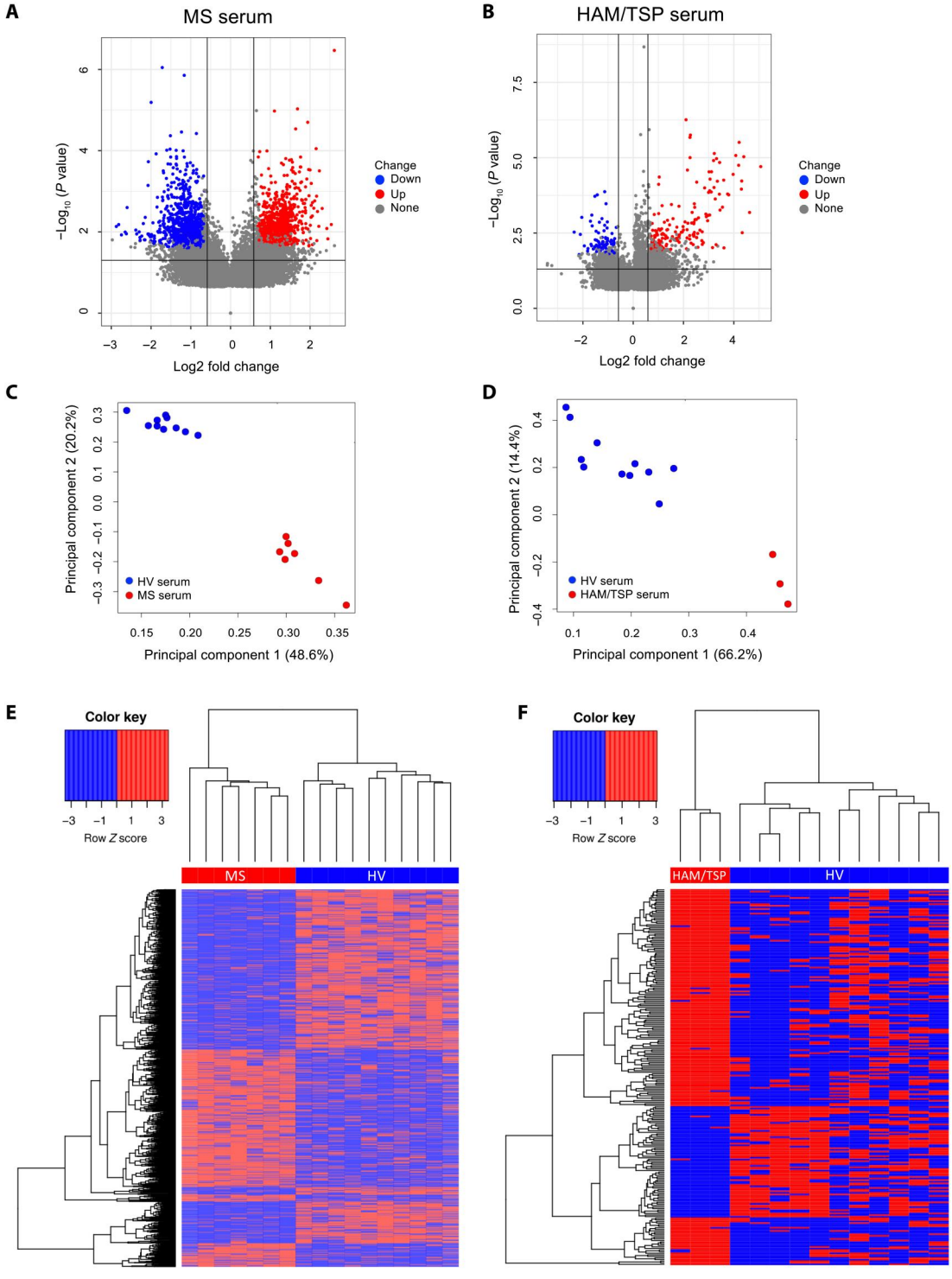

Fig. 3. Differential antibody profiles in serum between patients with MS and HVs. (**A** and **B**) Volcano plots showing significant fold changes of antibodies against viral peptide tiles in serum of patients with MS (A) and patients with HAM/TSP (B) compared to HVs. (**C** and **D**) PCA plot showing the significant differences of antibodies against viral peptide tiles in serum of patients with MS (C) and patients with HAM/TSP (D) compared to HVs. (**E** and **F**) Combined heatmap with cluster analysis showing the significant differences of antibodies against viral peptide tiles in serum of patients with MS (E) and patients with HAM/TSP (F) compared to HVs.

viral species are observed, including 42 peptide tiles for EBV (table S8). Twenty-eight of these 42 EBV peptide tiles have greater counts in serum of patients with MS compared to HVs (table S8). For the 237 viral peptide tiles comprising the HAM/TSP signature in serum, a total of 70 viral species are represented including PTLV, EBV, and CMV (table S9). Patients with MS could be correctly classified 91.67% of the time by machine learning under LOOCV conditions to the MS signature in serum (fig. S3). Larger sample numbers will be needed to support these classifications.

VirScan is a powerful approach for analyzing CSF antibody-repertoire profiles of all known human viruses. Using VirScan as a virus-discovery tool, it is possible to identify a single causative virus with disease specificity as reported previously (*9*, *13*) and as we demonstrate here in patients with HAM/TSP where we show specific increases in serum and CSF antibodies to PTLVs compared to HVs or patients with MS. Applying the identical virus discovery pipeline (*6*) in our cohort of patients with MS, we can confirm that patients with MS showed increased serum and now CSF antibody responses to EBV peptide tiles consistent with the known reports of increased EBV antibody responses in MS (*18*). However, patients with another chronic, progressive neuroinflammatory disease, HAM/TSP, also showed increased serum and CSF antibody responses against EBV and CMV. In patients with HAM/TSP, elevated antibody-secreting B cells have been reported to be significantly correlated with increased activated T cells with increased HTLV-1 viral load in the CSF (*17*). Similar to MS, several abnormalities in B cells including cytokine productions and interaction with T cells and EBV-specific antibody responses in CSF have been reported (*19*), but the mechanism that underlies B cell dysregulation and EBV involvement remains unknown. Since reactivation of ubiquitous viruses and the associated immune reactivation have been demonstrated in various neurologic diseases (*20*), immune reactivation against EBV and other ubiquitous human herpesviruses may be partially involved in neuroinflammatory diseases associated with T and B cell dysfunction. Rather than using VirScan with a virus discovery analysis methodology, which did not show an MS disease-specific increase in immunoreactivity against EBV in serum and CSF, we used a viral signature pipeline that revealed a disease-specific antibody signature in CSF and serum of patients with MS. Our findings suggest that antibody responses against multiple viral peptides, including EBV, can be identified. Rather than a single causative agent that has long been elusive to prove in a disease like MS, antibody profiling may better represent a virological exposure history that suggests multiple triggers potentially cross-reactive with self-peptides associated with immune-mediated neuroinflammatory disease (*21*). Since regulation of the local immune response is crucial in protecting the CNS from viral infection and immune-mediated tissue damage, CSF antibody profiling, including quantity and quality, would be influenced by immunopathogenic processes associated with viral infection and autoimmune disease. Therefore, larger patient cohorts will be required to determine whether these antibody profiles are disease-specific or predictive of a disease outcome.

MATERIALS AND METHODS

Subjects

The samples of a total of 12 HVs, 13 patients with relapsing remitting MS, and 3 patients with HAM/TSP were used for the study (table S1). Patients with MS and those with HAM/TSP were evaluated according to the diagnostic criteria and the established World Health Organization criteria, respectively. HTLV-1–uninfected healthy volunteers screened at the NIH Clinical Center (Bethesda, MD, USA) were evaluated as HVs. Serum and the paired CSF samples were collected from the subjects at visit. Sera were prepared from blood samples and then stored in a −80°C freezer until use. CSF was obtained by lumbar puncture. The CSF supernatants were collected within an hour by centrifugation and stored in a −80°C freezer until use. The study protocols (89-N-0045, 98-N-0047, and 16-N-0058) were reviewed and approved by the National Institute of Neurological Disorders and Stroke Institutional Review Board. Before study inclusion, written informed consent was obtained from all the participants in accordance with the Declaration of Helsinki.

VirScan

Library preparation

A T7 phage library displaying 105,362 epitopes from 206 virus species was amplified with the plate method as previously described (*9*). Briefly, the host BLT5403 *Escherichia coli* bacteria were thoroughly mixed with T7 phage library in top agar and spread onto 15-cm LB plates. The phage was washed off the plates and collected with phage extraction buffer (20 mM tris-HCl, pH 8.0, 100 mM NaCl, and 6 mM $MgCl_2$) when bacteria on the plates are cleared by phage. Phage titer was determined by plate plaque assay and sequenced to confirm the epitope abundance.

PhIP-seq

Sera or CSF samples containing 2 μg of total IgG were mixed with 2 × 10^{10} plaque-forming units of phage library and protein A/G Dynabeads (Thermo Fisher Scientific) for 4 hours at 4°C in duplicate. A pre-IP "input" sample was also prepared along with six "beads-only" samples per assay in duplicate (i.e., those with no sera/CSF). The protein A/G beads were then precipitated by a magnet and washed three times with wash buffer and eluted in 40 μl of water. This eluant was then used in library preparation for sequencing. The amplified and indexed sequencing libraries were pooled and sequenced on an Illumina NextSeq 500 platform (50 bp, single end). Sequencing of the libraries was performed at the National Cancer Institute Center for Cancer Research Frederick Sequencing Core Facility. Sequencing depth is 1 million reads per sample, with a mapping rate higher than 90%.

Statistical pipeline

Viral discovery pipeline

Raw sequence files generated per sample were quality-inspected using the "FastQC" tool (https://www.bioinformatics.babraham.ac.uk/projects/fastqc/) and the results were evaluated across samples using the "MultiQC" tool (https://multiqc.info/). To remove the adaptor sequence present and trim remove low-quality sequence, the "Trimmomatic" tool (http://usadellab.org/cms/?page=trimmomatic) was used under default settings. Alignment of the postadaptor clipped and low-quality trimmed sequences against the VirScan2 reference (*9*) was accomplished using bowtie (http://bowtie-bio.sourceforge.net/manual.shtml) under specific conditions (-n 3 -l 30 -e 1000 --tryhard --nomaqround --norc --best --sam --quiet). Alignment files produced were sorted and indexed using the SAMtools "sort" and "index" commands, respectively (http://htslib.org/), and counts per viral

peptide tile per sample were enumerated using the "idxstats" command. To merge counts by viral peptide tile across sample duplicates, the phip-stat "merge-columns" command was used (https://github.com/lasersonlab/phip-stat). To generate zero-inflated *P* values per viral peptide tile per sample, the phip-stat "normalize-counts" and "gamma-Poisson-model" commands were applied to the counts observed by sample in conjunction with those observed for the pre-IP input sample. Inspection of the viral peptide tile counts for the pre-IP input sample (fig. S1) revealed that they are uniform; supporting the phage library used was not only of good quality but that the use of these counts as part of generating zero-inflated *P* values will effectively correct for false epitope variation without bias. These zero-inflated *P* values were then imported into R (https://cran.r-project.org/) and analyzed using a workflow previously published (*6*).

Viral exposure signature pipeline

Analytical pipeline for antibody profiling in CSF and serum between patients with MS or HAM/TSP and HVs is summarized in fig. S2. Sequences used for alignment in Viral Discovery Analysis were taken and aligned to the same VirScan2 reference using bowtie2 instead of bowtie (http://bowtie-bio.sourceforge.net/bowtie2/manual.shtml). Alignment files produced were processed the same as those for Viral Discovery Analysis up to but not including the generation of *Z* scores. Instead, the merged counts by viral peptide tile across sample duplicates were imported into R and then pedestalled by two and log (base = 2) transformed. After transformation, values were normalized by sample duplicate using the "cpm" command supported in the "edgeR" package. Sample duplicate data at this point were then organized into four subsets: (i) MS CSF versus HV CSF, (ii) HAM/TSP CSF versus HV CSF, (iii) MS serum versus HV serum, and (iv) HAM/TSP serum versus HV serum. For each subset, cyclic loess was applied to correct for differences in distribution spread and location across sample duplicates using the "normalizeBetweenArrays" command supported in the "limma" package. Sample duplicates, by subset, were then quality-inspected using the postnormalized values per viral peptide tile via a Tukey box plot, a covariance-based PCA scatterplot, and a correlation-based heatmap. If any sample duplicates presented as outliers, they were removed and normalization for the respective subset was repeated. Locally weighted scatterplot smoothing (Lowess) modeling of the normalized data by sample duplicate class (coefficient of variation ~ mean) was then performed by subset, and the fits were overplotted for inspection. The lowest mean value across the fits at which the linear relationship with coefficient of variation was grossly lost was defined as the noise threshold for the data. Viral peptide tiles not having a value greater than this threshold for at least one sample duplicate were discarded as noise-biased. Surviving viral peptide tiles having a value less than the threshold were floored to equal the threshold. Viral peptide tile values across sample duplicates were then collapsed by taking the mean. Differences between sample classes by viral peptide tile were tested under LOOCV conditions while correcting for differences in age and gender. Specifically, ANCOVA was applied per viral peptide tile under Benjamini-Hochberg false discovery rate multiple comparison correction conditions with Akaike information criterion step optimization. Viral peptide tiles observed to have a corrected type III *P* value <0.05 by this test with a linear fold difference of adjusted means ≥ 1.5× 100% of the time were deemed to be differential between the sample classes tested respectively. Confirmatory analysis using these viral peptide tiles was accomplished using the same methods described to inspect for outliers, while volcano plots were also generated to describe the number, magnitude, significance, and direction of the viral peptide tiles identified differential per sample class comparison. To explore and demonstrate the classification utility of the differential viral peptide tiles identified, those for subset (i) and separately for subset (iv) were modeled under LOOCV conditions using Elastic Net machine learning (figs. S3 and S4). Specifically, for each subset, a sample was "left out" and the "cv.glmnet" command was applied using an $\alpha = 0.3$ for subset (i) and an $\alpha = 0.9$ for subset (iv). The resulting models were then used to classify the sample not modeled and the process was repeated until each sample of each subset was left out once. Classification performance over all modeling rounds was summarized by confusion matrix using the "ggplot2" command, while coefficients for viral peptide tiles selected 100% of the time over all modeling rounds were summarized by a box-and-whisker plot.

Supplementary Materials

This PDF file includes:

Figs. S1 to S4
Tables S1 to S9

View/request a protocol for this paper from *Bio-protocol*.

REFERENCES AND NOTES

1. D. S. Reich, C. F. Lucchinetti, P. A. Calabresi, Multiple sclerosis. *N. Engl. J. Med.* **378**, 169–180 (2018).
2. A. Ascherio, K. L. Munger, Epidemiology of multiple sclerosis: From risk factors to prevention-an update. *Semin Neurol.* **36**, 103–114 (2016).
3. S. Cepok, B. Rosche, V. Grummel, F. Vogel, D. Zhou, J. Sayn, N. Sommer, H. P. Hartung, B. Hemmer, Short-lived plasma blasts are the main B cell effector subset during the course of multiple sclerosis. *Brain* **128**, 1667–1676 (2005).
4. S. L. Hauser, E. Waubant, D. L. Arnold, T. Vollmer, J. Antel, R. J. Fox, A. Bar-Or, M. Panzara, N. Sarkar, S. Agarwal, A. Langer-Gould, C. H. Smith, B-cell depletion with rituximab in relapsing-remitting multiple sclerosis. *N. Engl. J. Med.* **358**, 676–688 (2008).
5. S. Tzellos, P. J. Farrell, Epstein-Barr virus sequence variation-biology and disease. *Pathogens* **1**, 156–174 (2012).
6. K. Bjornevik, M. Cortese, B. C. Healy, J. Kuhle, M. J. Mina, Y. Leng, S. J. Elledge, D. W. Niebuhr, A. I. Scher, K. L. Munger, A. Ascherio, Longitudinal analysis reveals high prevalence of Epstein-Barr virus associated with multiple sclerosis. *Science* **375**, 296–301 (2022).
7. T. V. Lanz, R. C. Brewer, P. P. Ho, J. S. Moon, K. M. Jude, D. Fernandez, R. A. Fernandes, A. M. Gomez, G. S. Nadj, C. M. Bartley, R. D. Schubert, I. A. Hawes, S. E. Vazquez, M. Iyer, J. B. Zuchero, B. Teegen, J. E. Dunn, C. B. Lock, L. B. Kipp, V. C. Cotham, B. M. Ueberheide, B. T. Aftab, M. S. Anderson, J. L. DeRisi, M. R. Wilson, R. J. M. Bashford-Rogers, M. Platten, K. C. Garcia, L. Steinman, W. H. Robinson, Clonally expanded B cells in multiple sclerosis bind EBV EBNA1 and GlialCAM. *Nature* **603**, 321–327 (2022).
8. T. W. Phares, S. A. Stohlman, C. C. Bergmann, Intrathecal humoral immunity to encephalitic RNA viruses. *Viruses* **5**, 732–752 (2013).
9. G. J. Xu, T. Kula, Q. Xu, M. Z. Li, S. D. Vernon, T. Ndung'u, K. Ruxrungtham, J. Sanchez, C. Brander, R. T. Chung, K. C. O'Connor, B. Walker, H. B. Larman, S. J. Elledge, Viral immunology. Comprehensive serological profiling of human populations using a synthetic human virome. *Science* **348**, eaaa0698 (2015).
10. T. P. Johnson, H. B. Larman, M. H. Lee, S. S. Whitehead, J. Kowalak, C. Toro, C. C. Lau, J. Kim, K. R. Johnson, L. B. Reoma, A. Faustin, C. A. Pardo, S. Kottapalli, J. Howard, D. Monaco, J. Weisfeld-Adams, C. Blackstone, S. Galetta, M. Snuderl, W. A. Gahl, I. Kister, A. Nath, Chronic dengue virus panencephalitis in a patient with progressive dementia with extrapyramidal features. *Ann. Neurol.* **86**, 695–703 (2019).
11. K. E. Leon, R. D. Schubert, D. Casas-Alba, I. A. Hawes, P. S. Ramachandran, A. Ramesh, J. E. Pak, W. Wu, C. K. Cheung, E. D. Crawford, L. M. Khan, C. Launes, H. A. Sample, K. C. Zorn, M. Cabrerizo, A. Valero-Rello, C. Langelier, C. Muñoz-Almagro, J. L. DeRisi, M. R. Wilson, Genomic and serologic characterization of enterovirus A71 brainstem encephalitis. *Neurol. Neuroimmunol. Neuroinflamm.* **7**, e703 (2020).

12. R. D. Schubert, I. A. Hawes, P. S. Ramachandran, A. Ramesh, E. D. Crawford, J. E. Pak, W. Wu, C. K. Cheung, B. D. O'Donovan, C. M. Tato, A. Lyden, M. Tan, R. Sit, G. M. Sowa, H. A. Sample, K. C. Zorn, D. Banerji, L. M. Khan, R. Bove, S. L. Hauser, A. A. Gelfand, B. L. Johnson-Kerner, K. Nash, K. S. Krishnamoorthy, T. Chitnis, J. Z. Ding, H. J. McMillan, C. Y. Chiu, B. Briggs, C. A. Glaser, C. Yen, V. Chu, D. A. Wadford, S. R. Dominguez, T. F. F. Ng, R. L. Marine, A. S. Lopez, W. A. Nix, A. Soldatos, M. P. Gorman, L. Benson, K. Messacar, J. L. Konopka-Anstadt, M. S. Oberste, J. L. DeRisi, M. R. Wilson, Pan-viral serology implicates enteroviruses in acute flaccid myelitis. *Nat. Med.* **25**, 1748–1752 (2019).
13. E. Shrock, E. Fujimura, T. Kula, R. T. Timms, I. H. Lee, Y. Leng, M. L. Robinson, B. M. Sie, M. Z. Li, Y. Chen, J. Logue, A. Zuiani, D. McCulloch, F. J. N. Lelis, S. Henson, D. R. Monaco, M. Travers, S. Habibi, W. A. Clarke, P. Caturegli, O. Laeyendecker, A. Piechocka-Trocha, J. Z. Li, A. Khatri, H. Y. Chu; MGH COVID-19 Collection & Processing Team, A. C. Villani, K. Kays, M. B. Goldberg, N. Hacohen, M. R. Filbin, X. G. Yu, B. D. Walker, D. R. Wesemann, H. B. Larman, J. A. Lederer, S. J. Elledge, Viral epitope profiling of COVID-19 patients reveals cross-reactivity and correlates of severity. *Science* **370**, eabd4250 (2020).
14. J. Liu, W. Tang, A. Budhu, M. Forgues, M. O. Hernandez, J. Candia, Y. Kim, E. D. Bowman, S. Ambs, Y. Zhao, B. Tran, X. Wu, C. Koh, P. Surana, T. J. Liang, M. Guarnera, D. Mann, M. Rajaure, T. F. Greten, Z. Wang, H. Yu, X. W. Wang, A viral exposure signature defines early onset of hepatocellular carcinoma. *Cell* **182**, 317–328.e10 (2020).
15. M. Puccioni-Sohler, Y. Yamano, M. Rios, S. M. F. Carvalho, C. C. F. Vasconcelos, R. Papais-Alvarenga, S. Jacobson, Differentiation of HAM/TSP from patients with multiple sclerosis infected with HTLV-I. *Neurology* **68**, 206–213 (2007).
16. S. Nozuma, S. Jacobson, Neuroimmunology of human T-lymphotropic virus type 1-associated myelopathy/tropical spastic paraparesis. *Front. Microbiol.* **10**, 885 (2019).
17. Y. Enose-Akahata, S. Azodi, B. R. Smith, B. J. Billioux, A. Vellucci, N. Ngouth, Y. Tanaka, J. Ohayon, I. Cortese, A. Nath, S. Jacobson, Immunophenotypic characterization of CSF B cells in virus-associated neuroinflammatory diseases. *PLOS Pathog.* **14**, e1007042 (2018).
18. A. Bar-Or, M. P. Pender, R. Khanna, L. Steinman, H. P. Hartung, T. Maniar, E. Croze, B. T. Aftab, G. Giovannoni, M. A. Joshi, Epstein-Barr virus in multiple sclerosis: Theory and emerging immunotherapies. *Trends Mol. Med.* **26**, 296–310 (2020).
19. R. W. Jain, V. W. Yong, B cells in central nervous system disease: Diversity, locations and pathophysiology. *Nat. Rev. Immunol.* **22**, 513–524 (2021).
20. J. Wouk, D. Z. Rechenchoski, B. C. D. Rodrigues, E. V. Ribelato, L. C. Faccin-Galhardi, Viral infections and their relationship to neurological disorders. *Arch. Virol.* **166**, 733–753 (2021).
21. J. E. Libbey, L. L. McCoy, R. S. Fujinami, Molecular mimicry in multiple sclerosis. *Int. Rev. Neurobiol.* **79**, 127–147 (2007).

Acknowledgments

Funding: This research was supported by the Intramural Research Program of the NINDS, NIH. The support of the NIH inpatient and outpatient neurology staff is acknowledged. L.W. and X.W.W. were supported by the Intramural Research Program of the Center for Cancer Research, NCI, NIH. This work used the computational resources of the NIH HPC Biowulf cluster (http://hpc.nih.gov). This research was supported by the Intramural Research Program of the NINDS, NIH and also supported by the Intramural Research Program of the Center for Cancer Research, NCI, NIH. **Author contributions:** Conceptualization: Y.E.-A. and S.J. Coordination of clinical work: Y.M. and J.O. Methodology: L.W., F.A., and K.R.J. Investigation: L.W., F.A., and K.R.J. Visualization: Y.E.-A., F.A., and K.R.J. Supervision: X.W.W. and S.J. Writing—original draft: Y.E.-A., L.W., F.A., and K.R.J. Writing—review and editing: Y.E.-A., L.W., F.A., K.R.J., X.W.W., and S.J. **Competing interests:** The authors declare that they have no competing interests. **Data and materials availability:** All data needed to evaluate the conclusions in the paper are present in the paper and/or the Supplementary Materials.

Submitted 25 April 2022
Accepted 30 November 2022
Published 4 January 2023
10.1126/sciadv.abq6978